

Spiker: an FPGA-optimized Hardware accelerator for Spiking Neural Networks

Alessio Carpegna
Control and Computer Eng. Dep.
Politecnico di Torino
Torino, Italy
alessio.carpegna@polito.it

Alessandro Savino
Control and Computer Eng. Dep.
Politecnico di Torino
Torino, Italy
alessandro.savino@polito.it

Stefano Di Carlo
Control and Computer Eng. Dep.
Politecnico di Torino
Torino, Italy
stefano.dicarlo@polito.it

Abstract—Spiking Neural Networks (SNN) are an emerging type of biologically plausible and efficient Artificial Neural Network (ANN). This work presents the development of a hardware accelerator for a SNN for high-performance inference, targeting a Xilinx Artix-7 Field Programmable Gate Array (FPGA). The model used inside the neuron is the Leaky Integrate and Fire (LIF). The execution is clock-driven, meaning that the internal state of the neuron is updated at every clock cycle, even in absence of spikes. The inference capabilities of the accelerator are evaluated using the MNIST dataset. The training is performed offline on a full precision model. The results show a good improvement in performance if compared with the state-of-the-art accelerators, requiring $215\mu s$ per image. The energy consumption is slightly higher than the most optimized design, with an average value of $13mJ$ per image. The test design consists of a single layer of four-hundred neurons and uses around 40% of the available resources on the FPGA. This makes it suitable for a time-constrained application at the edge, leaving space for other acceleration tasks on the FPGA.

Index Terms—Spiking Neural Networks, LIF, MNIST, FPGA, Neuromorphic accelerator

I. INTRODUCTION

Artificial Neural Networks (ANNs) are complex computational learning models that often exploit the computing power of enterprise data centers and public cloud infrastructures to speed up training and inference. However, the cloud-based ANN model is showing its limitations [1]. Moving a large amount of data through the Internet implies a considerable energy overhead spread along the communication channel. Communication means a non-negligible latency, not compatible with performance-constrained applications (e.g., real-time systems). This may create a severe bottleneck with the increasing pervasiveness of the Internet of Things (IoT) that risks saturating the network communication towards centralized servers [2]. Finally, there are applications in which, for security reasons, data must be kept local.

All these factors push toward moving part of the ANN processing, if not all, towards the edge of the network, closer to where the data originated and where responses are required. However, when ANNs are deployed at the edge, they cannot feature the same computing power as in the cloud, where high-performance GPUs and computing cores are available. Specialized accelerators can cover this gap to speed up ANN inferencing at the edge [3]. Nevertheless, hardware accelera-

tion alone is not enough to fully benefit from the power of ANNs at the edge. Learning models must be adapted to this new limited environment.

In Convolutional Neural Networks (CNNs), one of the dominant ANN models, each neuron requires many calculations (mainly multiplying and accumulating) at every cycle. This creates a pattern suitable for massively parallel implementations but wastes resources. Moreover, if the goal of ANNs is to mimic the behavior of the human brain, this model is far from its biological counterpart. Spiking Neural Networks (SNN), an emerging type of event-based neural network, can make a difference in this sense [4]. In an SNN, the information between neurons is exchanged in form of binary spikes, thus minimizing resources to link neurons in the network. Additionally, time is treated as an additional dimension in the input and this makes SNNs more suitable for processing time series.

In the past, SNNs were mainly implemented on CPUs using software frameworks such as Brian/Brian2 [5] or in GPU-based frameworks such as CARLsim4 [6]. Since these computing architectures cannot efficiently support the sparse feature of SNNs, specific ASIC processors have been proposed, e.g., TrueNorth from IBM [7] or SpiNNaker [8]. When hardware resources are limited, Field Programmable Gate Arrays (FPGAs) offer a great technology to implement several accelerators on the same hardware block to speed up different tasks thanks to their in-field programmability [9, 10, 11, 12, 13, 14]. However, the existing designs still face a complexity that may prevent the deployment of extensive networks at the edge.

This paper presents Spiker, a new FPGA-based SNN hardware accelerator with off-line training based on the well-known Leaky Integrate and Fire (LIF) neuron model. Spiker aims to reduce at a minimum the size of the architecture, with the specific goal of maximizing the allowed parallelism, reducing the required execution time to fit performance-constrained applications at the edge. This is obtained by introducing well-crafted approximations, reducing the size of the neuron. The target dataset used to evaluate the designed accelerator is the MNIST [15]. The training is performed offline with a full precision model, using the Spike Timing Dependent Plasticity (STDP) unsupervised learning method [16]. In contrast, the

inference is performed on the accelerator with the simplified neuron structure. Experimental results show that this simplified model introduces a slight accuracy loss compared to the full precision counterpart, provides high throughput, and maintains low hardware complexity.

II. BACKGROUND

Spiking neural networks have first emerged in computational neuroscience to model the behavior of biological neurons. The body of a neuron (Figure 1-a), also called soma, is characterized by an internal state associated with a voltage across its membrane (i.e., membrane potential). Stimuli (i.e., signal spikes) received at the input terminals of the neuron (i.e., dendrites) can modify the membrane potential. In particular excitatory stimuli cause an increment in the membrane potential, while inhibitory stimuli decrease it. If the potential exceeds a threshold, an action potential takes place. The action potential is a sudden increase in the membrane voltage, which then rapidly tends towards its rest value [17]. This generates a voltage spike propagating to other neurons through the output terminals (i.e., axons).

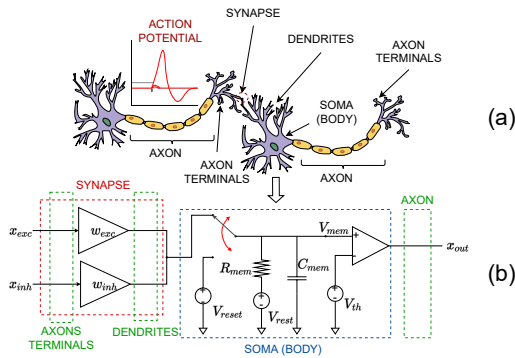


Fig. 1. SNN neuron concept: (a) biological structure, (b) equivalent circuit of the LIF model.

Many mathematical models have been developed in the last decade to quantitatively describe this kind of behavior. The Hodgkin-Huxley model is the most accurate and precisely describes the behavior of ions within the membrane [18]. It is very realistic but too complex for hardware implementations. The Izhikevich model exploits mathematical properties to simplify the Hodgkin-Huxley model [19], and some works use this model in hardware accelerators [20]. However, our architecture aims to reduce the area occupation, and the Izhikevich model is too complex to accomplish this goal. The simplest available model is the Integrate and Fire (IF) model, which treats the membrane as an ideal capacitance. However, this model is too approximated and leads to behaviors quite different from those observed in a biological neuron. Eventually, the Leaky Integrate and Fire (LIF) model is a good trade-off between simplicity and biological realism.

The LIF model treats the membrane as a leaky capacitance, including a resistive part that forces the voltage towards a rest value in the absence of input stimuli. The temporal evolution

of the membrane potential can be described through the characteristic equations of the LIF equivalent circuit (Figure 1-b). Equation 1 governs the membrane potential $V(t)$, where V_{rest} is the resting potential in the absence of stimuli, t_0 is the initial time (e.g., the instant in which the neuron receives a spike), and τ is the time constant of the equivalent RC-circuit, namely $\tau = R_{mem} \cdot C_{mem}$.

$$\frac{dV(t)}{dt} = \frac{1}{\tau} \cdot (V_{rest} - V(t_0)) \quad (1)$$

Solving the differential equation leads to an exponential evolution of the membrane potential in the form of:

$$V(t) = V_{rest} + (V(t_0) - V_{rest}) \cdot e^{-\frac{t-t_0}{\tau}} \quad (2)$$

A specific conductance acting as a weight characterizes each synapse, i.e., the interface between the dendrites and axons of two neurons. The conductance modifies the incoming spikes, leading to a variation in the membrane potential proportional to the synapse's weight. This conductance-based model is complex despite being a faithful emulation of biological behavior. A simpler alternative is the current-based synapse model. In this case, the synapse is treated as a simple charge amplifier. The input arrives in the form of an ideal current spike that affects the membrane potential proportionally to the charge it delivers.

Spike-timing-dependent plasticity (STDP) is among the most used learning algorithms in SNNs [16]. This biologically inspired learning rule modifies the synaptic strength (i.e., weights) as a function of the relative timing of pre- and post-synaptic spikes. The details of the learning procedure are not reported in this work since the accelerator has been designed for inference. The user is free to decide the training method enabling reaching the desired goal, such as accuracy or biological plausibility.

III. ARCHITECTURE

This section overviews the general architecture of Spiker (Figure 2). It focuses on the optimizations introduced to reduce the hardware complexity and improve performance. Overall, Spiker includes an input and an output layer used to interface the spiking core of the network with the external data and several hidden layers processing spikes. Spiker implements a clock-driven neuron architecture, i.e., in the absence of spikes, the membrane potential is updated at every clock cycle following the exponential trend reported in Equation 2. However, inputs are processed only when at least one spike is present at the input of a layer. This solution is more power-hungry than pure event-driven architectures but allows reducing the required hardware resources to a minimum. Finally, the architecture works with fixed-point arithmetic.

A. Input interface

SNNs process numerical data vectors that must be converted into sequences of spikes. Spikes are represented as single bits in the digital domain to minimize resources. There are different methods available for this conversion, depending on the type of input data [21]: (i) firing rate coding (i.e., information

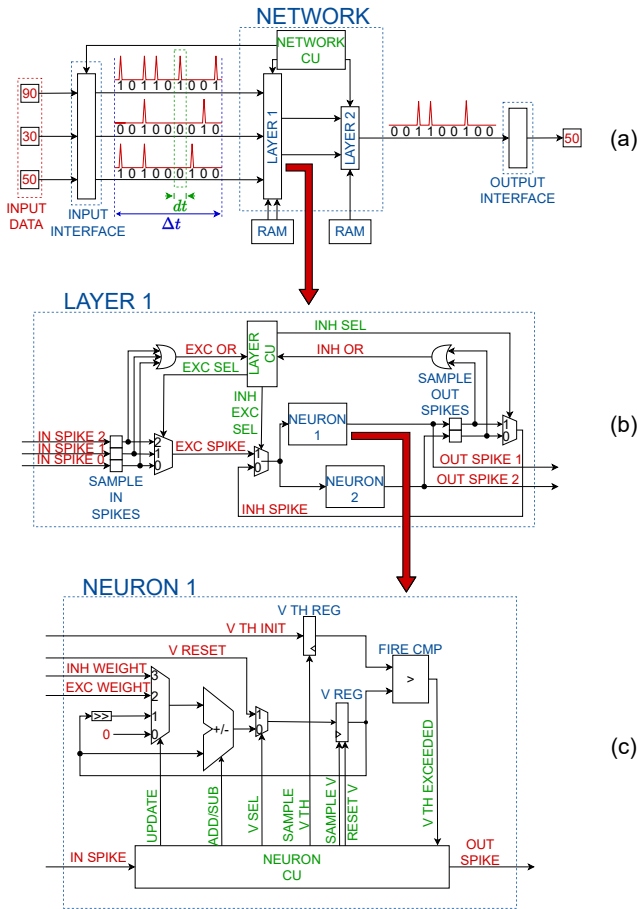


Fig. 2. Network architecture

is encoded using the instantaneous average firing rate), (ii) population rank coding (i.e., information is encoded using the relative firing time of a population of neurons), or (iii) temporal coding (i.e., information is encoded with the exact timing of individual spikes). Temporal encoding is the most biologically realistic encoding suited for dynamically evolving data. Nevertheless, Spiker uses firing rate coding that works well for static data such as images and enables compact and optimized hardware implementation.

In Spiker, one input data (e.g., the intensity of a pixel in an image) is treated as an instantaneous firing rate (i.e., the probability that a spike occurs within an interval). The conversion process starts selecting the duration of the spike sequence (Δt in Figure 2-a) that is the same for all inputs. The sequence is split into computation steps of duration dt , each able to accommodate a single spike. This parameter defines the temporal resolution of the network. The product of the numerical input (*rate*) by dt provides the average number of spikes $ASPS = \text{total spikes}/\text{total steps} = \text{rate} \cdot dt$ that must be generated in each step of the whole spike sequence. $ASPS$ is a number between zero and one since one spike per step can occur at most. The conversion process finally requires generating a random number n between zero and one. If n is greater than $ASPS$, a spike takes place. This method allows

generating a random sequence of statistically independent spikes whose timing follows a Poisson distribution [22].

This approach requires the generation of random values both during training and inference. During training (performed off-line), a statistically independent random value is generated for each network input. This guarantees high accuracy, leading the network to generalize the input patterns better. However, Spiker uses a single random value for all input data in parallel once the network has been trained. This strongly reduces the hardware cost with a negligible effect on the accuracy during inference. The generation of a pseudo-random value on-board uses a Linear Feedback Shift Register (LFSR). The substantial area reduction introduced by the use of a single LFSR for all inputs allows to increase the period of the generated random sequence, equal to $2^{\text{bit-width}}$ in a maximal LFSR, thus improving the quality of the random numbers with a negligible impact on the global area.

B. Output interface

The output interface translates the sequences of spikes generated at the network's output into numerical information that can be further processed. Spiker implements this interface using simple counters, one for each output neuron. The value of these counters should be normalized by the duration of the spike sequence (Δt) to obtain the firing rate of the output neurons. However, being Δt the same for all neurons, this operation can be avoided, thus saving area. The computed firing rates can then be used to infer, for example, by looking at which neuron has been the most active for a specific input pattern.

C. Network architecture

The network can be composed of an arbitrary amount of layers, connected in a feed-forward structure (Figure 2a). A central control unit (CU) manages the elaboration that is organized into temporal steps. When all the layers are ready, the CU orders the input interface to generate a new set of spikes, corresponding to one temporal step dt . The spikes are generated in parallel for all the inputs. Then the CU enables all layers in parallel to start a new elaboration on the inputs. The first layer takes directly the input spikes. All the others use the output generated by the corresponding previous layer as an input. In this way the information is propagated in the feed-forward direction in a sort of pipeline.

When a layer ends its computation, it informs the central CU that it is ready and then waits. Since elaboration in different layers can take different time, the main CU waits for all layers to finish and then starts a new elaboration cycle. This process is repeated until the entire sequence of input spikes is elaborated.

D. Layer

A layer (Figure 2-b) can be composed of an arbitrary number of neurons, updated in parallel. A dedicated layer CU manages the elaboration. In particular, in Spiker, each neuron can elaborate one spike at a time. The first role of the layer

CU is to provide the input spikes one-by-one to all the neurons in parallel.

Spiker gives the possibility to implement inter-layer inhibitory connections. Each neuron can be connected to all the other neurons of the layer using links with negative weights. This creates an inhibitory effect that reduces their membrane potential, preventing a neuron from firing a spike. The layer control unit also manages the elaboration of the spikes coming from inhibitory connections. The process is the same seen for the excitatory connections. The spikes are sampled in parallel, and then, once the elaboration of the excitatory spikes ends, the control unit switches to the inhibitory ones providing them one-by-one to all the neurons.

Since spikes are elaborated one by one, a complete update cycle can take considerable time. One of the advantages of the SNNs is that, if the model and the input encoding are well designed, the spike sequences received and generated are pretty sparse. To evaluate this characteristic, a statistical analysis is performed considering the MNIST dataset used in section IV in our experimental setup. The goal is to verify how many steps dt within the sequence Δt contain at least one active spike.

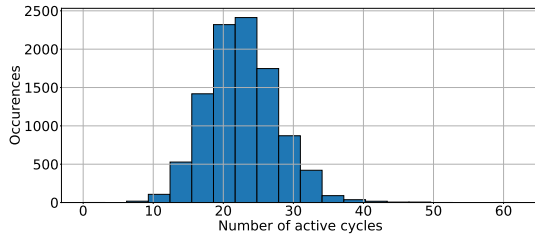


Fig. 3. Statistics of the active elaboration steps (i.e., cycles with at least one spike) on all images of the MNIST dataset. Obtained values have been computed with a window of 3,500 elaboration steps.

Figure 3 shows that, on average, twenty-three steps are active on a total of 3,500, which corresponds to less than the 1%. A similar result has been obtained for the inhibitory spikes. Spiker uses this characteristic to improve its performance. In all steps without active spikes, performing computations would be a waste of time and power. A simple OR operation applied on all spikes (both excitatory and inhibitory) enables Spiker to skip the elaboration in all steps without active spikes.

E. Neuron

The architecture of the neuron is minimal (Figure 2-c). This is the strong point of the designed accelerator. Being the architecture clock-driven, the exponential decay, corresponding to Equation 1, is solved as:

$$V[n] = V[n-1] + \frac{dt}{\tau} \cdot (V_{rest} - V[n-1]) \quad (3)$$

Here is where the two main optimizations are performed. First, the internal voltage parameters, that are the rest potential, the reset potential and the threshold, are moved, using an offset, in order to obtain $V_{rest} = 0V$. This simplifies Equation 3 to:

$$V[n] = V[n-1] - \frac{dt}{\tau} \cdot V[n-1] \quad (4)$$

thus removing the need to add V_{rest} , reducing the required computations by one. See section IV for a practical example.

Second, the equation still involves a multiplication ($\frac{dt}{\tau} \cdot V[n-1]$), which requires a lot of hardware resources. To avoid it the quantity $\frac{dt}{\tau}$ is approximated to the nearest negative power of two. In this way the multiplication can be substituted with a simple bit shift, which can be computed with zero cost in terms of hardware components. The advantage of such an approximation is that, if the model is designed properly, so choosing dt and τ such to make their ratio equal or near to a negative power of two already in the training phase, the approximation has no, or at least a small, impact on the accuracy.

The other operations that the neuron can perform are: (i) resetting the membrane potential to V_{reset} when it exceeds the threshold, forcing it to $V_{rest} = 0V$ (through the synchronous reset signal RESET V) at the end of the complete elaboration in order to start all the elaborations from the same state, and (ii) add an excitatory or inhibitory weight to the membrane potential when an active spike is received.

Finally, one additional advantage of the designed structure is that it allows initializing the threshold to an arbitrary value, which can be different for all the neurons. This provides the freedom to use it as an additional hyperparameter that can be tuned for each neuron during the learning phase.

F. Weights memory

The memory required by the weights is generally too big to fit into the flip-flops available in an average FPGA. For this reason, Spiker stores the weights in an external memory. In this case, the access parallelism of the memory becomes the main performance bottleneck since it determines how many weights can be accessed, and so how many neurons can be updated in parallel. Many FPGAs, like the one used in this paper (see section IV), are equipped with Block RAM (BRAM). A BRAM is a memory, divided into blocks that are directly integrated within the FPGA. The blocks can be accessed in parallel, enabling a high degree of parallelism in the accelerator. Quantization of the weights is performed to reduce the required bit-width to a minimum, thus reducing the memory occupation and increasing the number of weights that can be accessed in parallel with the same memory bandwidth.

While processing the spikes sequentially, the layer provides the index of the currently analyzed spike as an output. A dedicated circuit is then required to translate such an index to the physical address for all the BRAMs that must be accessed in parallel.

IV. EXPERIMENTAL RESULTS

A. Experimental set-up

Spiker has been tested on the MNIST dataset, a database of 28x28 grey-scale images with eight-bit per pixel. The SNN network developed by Diehl and Cook [23] is taken as a

reference. Table I summarizes the original parameters of the model and the values used in Spiker after shifting V_{rest} to 0mV (i.e., a shift of 65.0mV) as proposed in subsection III-E. The evaluation of the accelerator is performed using the whole test set, composed of 10,000 images.

TABLE I
OPTIMIZED MODEL PARAMETERS

Parameter	Original Value	Used Value
V_{rest}	-65.0mV	0mV
V_{reset}	-60.0mV	5.0mV
V_{th0}	-52.0mV	13.0mV
τ	100ms	-
w_{inh}	-15	-15
Δt	350ms	350ms
δt	0.1ms	0.1ms
Cycles	3500	3500
$\frac{\delta t}{\tau}$	$\frac{0.1ms}{100ms} = 10^{-4}$	2^{-10}

According to the reference model, the parameters are tuned for a network structure with 400 neurons and inhibitory connections between the neurons. This structure allows reaching acceptable accuracy results, even if non-optimal, as seen in the dedicated section, with a total number of neurons reasonable to integrate on an average FPGA. It is important to remark here that the goal of the evaluation is not to show the superiority of this model compared to other neural networks (e.g., CNNs). This model was selected since it is used in other studies proposing FPGA-based SNN hardware acceleration and allows us to compare Spikers with its competitors.

The network works with fixed-point precision. The bit-width used inside the neuron is set to 16 bit (3 fractional and 13 integer). Instead, the quantization of weights is down to 5 bit (3 fractional and 2 integers). The total memory required is therefore $400 \times 28 \times 28 \times 5$ bit = 196 KByte. The training is performed in full-precision using STDP on a custom python simulation of the model.

B. Accuracy results

Table II shows the effect of the neuron approximations introduced in Spiker on the accuracy of the network. The training accuracy is reported only for the reference and the Spiker LIF full precision models, since the training is always performed in full precision. The various simplifications are then applied only during inference, for which the accelerator is designed. Table II shows that:

- 1) Changing the model from a conductance-based [23] solution to a lighter current-based alternative has no significant impact on the training phase and implies a relatively small 1.42% reduction during inference.
- 2) Using a single random number generator in the input interface, (*Current-based 1 LFSR* in Table II), causes an additional 2.19% accuracy reduction.
- 3) Working with an internal parallelism of 16 bits and quantizing the weights down to a 5 bits width implies a further 1.01% accuracy decrease.

- 4) The approximation of the ration between δt and τ has no effect on the accuracy, since the starting value was quite near to 2^{-10} .

TABLE II
TRAINING AND TEST RESULTS WITH DIFFERENT SIMPLIFICATIONS

Model	Training	Inference
Peter Diehl[23]	80.54%	78.58%
Spiker LIF model full precision	80.22%	77.16%
Spiker LIF model 1 LFSR	-	74.97%
Spiker LIF model 16bit/5bit	-	73.96%

So the overall accuracy reduction of the completely simplified model, when compared to the reference one, is around 4.5%, which is more than acceptable considering the substantial hardware simplification.

C. Area and performance results

The designed accelerator has been synthesized on a medium-size Xilinx Artix-7 FPGA. All the four-hundred neurons are instantiated as physical components and can be updated in parallel. The available BRAM allows accessing all the required weights in parallel. The routing gives no issues.

TABLE III
REQUIRED AREA

HW component	LUT	FF	BRAM
Single neuron	62	40	-
400 neurons	23885	15614	-
Complete layer	26038	16846	-
Spikes generator	6343	6311	-
Weights	-	-	45
Complete accelerator	29145 (55%)	26853 (25%)	45 (32%)
Total FPGA Available	53200	106400	140

Table III shows the required hardware resources. The last row summarizes all the available components. Overall, the FPGA usage is around 55% for the LUTs, 25% for the FFs and 32% for the available memory. This is a significant result considering the high number of instantiated neurons.

D. Comparison with other accelerators

Table IV shows the comparison between different accelerators tested on MNIST. The table reports the key results to highlight the contributions of this work and to compare it to other similar works. Comparison is performed with accelerators based on the same neuron model (LIF) and targeting the same dataset (MNIST). For a fair comparison of the performance, the time required to elaborate an image is normalized, considering a working frequency of 100MHz for all the accelerators. The reported computation time for Spiker ($215\mu s$) is the fastest among the considered accelerators, demonstrating how all the design optimizations described before make the processing structures required for the computation simpler and more efficient. This result is also significant considering that the number of synapses that can be instantiated in the fastest competitor is half the number instantiated with Spiker. From the energy standpoint, while the

TABLE IV
COMPARISON TABLE

Design	[10]	[11]	[12]	[13]	This work
Clock frequency(MHz)	75	120	25	100	100
Data format	16bit Fixed	8bit Fixed	32bit Fixed	16bit Floating	16bit Fixed
Computing scheme	Event-Driven	Clock-Driven	Event-Driven	Adaptive Clock/Event-Driven	Clock-Driven
Neuron model	LIF	LIF	LIF	LIF	LIF
FPGA platform	Spartan 6	Virtex 6	Spartan 6	Virtex 7	Artix 7
Neurons	1794	1591	1794	1094	1384
Synapses	647000	638208	647000	177800	313600
Task	MNIST	MNIST	MNIST	MNIST	MNIST
Computation time	0.53s/image	8.40s/image	0.16s/image	3.15ms/image	215 μ s/image
Computation time @100MHz	0.40s/image	10.08s/image	40.00ms/image	3.15ms/image	215 μ s/image
Energy	0.80J/image	1.12J/image	Not reported	5.04mJ/image	13mJ/image
Energy/Synapse	1.2 μ J/synapse	1.76 μ J/synapse	Not reported	0.028 μ J/synapse	0.041 μ J/synapse

reported energy per image is twice the best design, i.e., [13], the energy per synapse makes the energy consumption almost comparable. Nevertheless, considering that the best competitor in terms of energy consumption relies on a mixed strategy that includes an event-driven part, this makes the developed architecture particularly promising. As a reference, the test of the model using Brian 2 [5] required 0.2s on a 2GHz Intel i5 dual-core processor.

V. CONCLUSIONS

This work presented Spiker, a small high-performance SNN hardware accelerator synthesized on a Xilinx Artix-7 FPGA and tested on the MNIST dataset. Spiker significantly accelerates inference, with a competitive energy consumption and a limited impact on the accuracy. Presented results are a good starting point for future work, in which different and deeper network structures will be considered. The main goal will be to improve the classification accuracy, making it comparable with other state-of-the-art accelerators. This, together with its competitive performance, can make Spiker a very good solution for performance-constrained applications at the edge.

REFERENCES

- [1] Alberto Marchisio et al. "Deep learning for edge computing: Current trends, cross-layer optimizations, and open research challenges". In: *2019 IEEE Computer Society Annual Symposium on VLSI (ISVLSI)*. IEEE, 2019, pp. 553–559.
- [2] Muhammad Shafique et al. "An overview of next-generation architectures for machine learning: Roadmap, opportunities and challenges in the IoT era". In: *2018 Design, Automation & Test in Europe Conference & Exhibition (DATE)*. IEEE, 2018, pp. 827–832.
- [3] Tianshi Chen et al. "Dianna: A small-footprint high-throughput accelerator for ubiquitous machine-learning". In: *ACM SIGARCH Computer Architecture News* 42.1 (2014), pp. 269–284.
- [4] Rachmad Putra et al. "FSpiNN: An optimization framework for memory-efficient and energy-efficient spiking neural networks". In: *IEEE Transactions on Computer-Aided Design of Integrated Circuits and Systems* 39.11 (2020), pp. 3601–3613.
- [5] Marcel Stimberg et al. "Brian 2, an intuitive and efficient neural simulator". In: *eLife* 8 (Aug. 2019), e47314. ISSN: 2050-084X.
- [6] Ting-Shuo Chou et al. "CARLsim 4: An open source library for large scale, biologically detailed spiking neural network simulation using heterogeneous clusters". In: *2018 International joint conference on neural networks (IJCNN)*. IEEE, 2018, pp. 1–8.
- [7] Filipp Akopyan et al. "Truenorth: Design and tool flow of a 65 mw 1 million neuron programmable neurosynaptic chip". In: *IEEE transactions on computer-aided design of integrated circuits and systems* 34.10 (2015), pp. 1537–1557.
- [8] Eustace Painkras et al. "Spinnaker: A multi-core system-on-chip for massively-parallel neural net simulation". In: *Proceedings of the IEEE 2012 Custom Integrated Circuits Conference*. IEEE, 2012, pp. 1–4.
- [9] Alessio Carpegna. "Design of an hardware accelerator for a Spiking Neural Network". Supervisors: Stefano Di Carlo, Alessandro Savino. MA thesis. Politecnico di Torino, Oct. 2021.
- [10] Daniel Neil and Shih-Chii Liu. "Minitaur, an Event-Driven FPGA-Based Spiking Network Accelerator". In: *IEEE transactions on very large scale integration (VLSI) systems* 22.12 (2014), pp. 2621–2628. ISSN: 1063-8210.
- [11] Qian Wang et al. "Energy efficient parallel neuromorphic architectures with approximate arithmetic on FPGA". In: *Neurocomputing (Amsterdam)* 221 (2017), pp. 146–158. ISSN: 0925-2312.
- [12] De Ma et al. "Darwin: A neuromorphic hardware co-processor based on spiking neural networks". In: *Journal of systems architecture* 77 (2017), pp. 43–51. ISSN: 1383-7621.
- [13] Sixu Li et al. "A Fast and Energy-Efficient SNN Processor With Adaptive Clock/Event-Driven Computation Scheme and Online Learning". In: *IEEE transactions on circuits and systems. I, Regular papers* 68.4 (2021), pp. 1543–1552.
- [14] Charlotte Frenkel et al. "A 0.086 – mm² 12.7-pJ/SOP 64k-Synapse 256-Neuron Online-Learning Digital Spiking Neuromorphic Processor in 28-nm CMOS". In: *IEEE transactions on biomedical circuits and systems* 13.1 (2019), pp. 145–158. ISSN: 1932-4545.
- [15] Li Deng. "The mnist database of handwritten digit images for machine learning research". In: *IEEE Signal Processing Magazine* 29.6 (2012), pp. 141–142.
- [16] Daniel E Feldman. "The Spike-Timing Dependence of Plasticity". In: *Neuron (Cambridge, Mass.)* 75.4 (2012), pp. 556–571. ISSN: 0896-6273.
- [17] Michael H. Grider, Rishita Jessu, and Rian Kabir. *Physiology, Action Potential*. 2021. URL: <http://europepmc.org/books/NBK538143>.
- [18] A. L Hodgkin and A. F Huxley. "A quantitative description of membrane current and its application to conduction and excitation in nerve". In: *The Journal of physiology* 117.4 (1952), pp. 500–544. ISSN: 0022-3751.
- [19] E.M Izhikevich. "Simple model of spiking neurons". In: *IEEE transactions on neural networks* 14.6 (2003), pp. 1569–1572. ISSN: 1045-9227.
- [20] Kit Cheung, S.R Schultz, and P.H.W Leong. "A parallel spiking neural network simulator". In: *2009 International Conference on iField-Programmable Technology*. IEEE, 2009, pp. 247–254. ISBN: 9781424443758.
- [21] Balint Petro, Nikola Kasabov, and Rita M. Kiss. "Selection and Optimization of Temporal Spike Encoding Methods for Spiking Neural Networks". In: *IEEE Transactions on Neural Networks and Learning Systems* 31.2 (2020), pp. 358–370.
- [22] David Heeger et al. "Poisson model of spike generation". In: *Handout, University of Stanford* 5.1-13 (2000), p. 76.
- [23] Peter U. Diehl and Matthew Cook. "Unsupervised learning of digit recognition using spike-timing dependent plasticity". In: *Frontiers in Computational Neuroscience* 9 (Aug. 2015). ISSN: 1662-5188.